Springer

KSME

Journal of Mechanical Science and Technology 24 (11) (2010) 2307~2313
www.springerlink.com/content/1738-494x
DOI 10.1007/s12206-010-0814-5

Design of safety mechanism for an industrial manipulator based on passive compliance †

Hwi-Su Kim[1], Jung-Jun Park[1], Jae-Bok Song[1,*] and Jin-Ho Kyung[2]

[1]*School of Mechanical Engineering, Korea University, Seoul, 136-713, Korea*
[2]*Korea Institute of Machinery and Materials, Daejeon, 305-343, Korea*

(Manuscript Received October 9, 2009; Revised June 17, 2010; Accepted August 6, 2010)

Abstract

In recent years, collision safety between humans and robots has drawn much attention since human-robot cooperation is increasingly needed in various fields. Since positioning accuracy and collision safety are both important, an industrial manipulator should maintain very high stiffness for positioning accuracy in a normal situation, but exhibit very low stiffness when subjected to a collision force greater than the tolerance for human injury. To satisfy these requirements, we proposed in our previous research a safety mechanism composed of a linear spring and a double-slider mechanism for a service robot with a small payload. We modified this device to meet more stringent requirements for an industrial manipulator which usually has a payload higher than a service robot. Several experiments on static and dynamic collisions showed high stiffness of the safety mechanism in response to an external torque that was less than a predetermined threshold torque, but low stiffness that enabled absorption of the collision force when the external torque exceeded the threshold. Thus, positioning accuracy and collision safety were improved using the proposed design. Furthermore, a new safety criterion is suggested to verify the collision safety of a manipulator that uses the proposed safety mechanism.

Keywords: Safe arm; Industrial manipulator; Safety mechanism; Collision safety

1. Introduction

In recent years, the potential for collisions between humans and robots has drawn much attention since human-robot cooperation is increasingly required in various fields of robotics. Furthermore, collision safety is very important for robots developed for small- and medium-sized enterprises, since these robot manipulators operate in the same space with workers.

Improving the safety of a robot arm can be achieved by either active compliance or passive compliance. In the actively compliant arm, collision is detected by a sensor, and the stiffness of a manipulator decreases by the appropriate control of a motor at each joint. Since this method requires force sensing for collision detection and actuation in response to a dynamic collision, its bandwidth is limited. Moreover, this approach suffers from measurement noise and possible malfunctions [1].

On the other hand, the passive compliance method consists of purely mechanical elements such as springs, links, cams, etc. Since this method does not use any sensor or actuator, it can provide fast and reliable responses, even for dynamic collision. Several mechanisms have been developed to improve safety using the passive compliance method; these include the mechanical impedance adjuster with a leaf spring and an electromagnetic brake [2], the programmable passive compliance shoulder mechanism [3], a variable system composed of a spring and a belt [4], and a passive compliance joint with rotary springs and a MR damper [5].

A spring is the most popular mechanical element for shock absorption. However, a spring used at the manipulator joint leads to positioning inaccuracy because displacement occurs even for a small external force that does not require any shock absorption. Although a hard spring can provide high positioning accuracy for a robot arm, its capability of shock absorption is much lower than a soft spring, thereby giving a higher probability of injury upon collision with humans.

To mitigate this problem, a safe link mechanism and a safe joint mechanism using a nonlinear spring system were suggested in our previous research [6, 7]. These safety mechanisms can exhibit very low stiffness when subjected to a collision force greater than that which may cause injury to humans, but can otherwise maintain a very high stiffness. However, since the implementation of this safety mechanism in an industrial manipulator requires higher capacity, the design of the safety mechanism should be modified.

† This paper was recommended for publication in revised form by Associate Editor Doo Yong Lee
* Corresponding author. Tel.: +82 2 3290 3363, Fax: +82 2 3290 3757
E-mail address: jbsong@korea.ac.kr

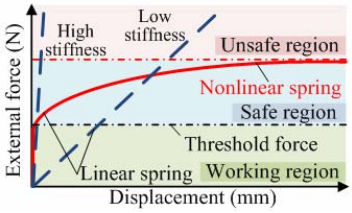

Fig. 1. Comparison between linear and nonlinear springs.

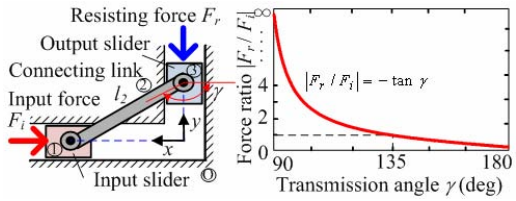

(a) (b)

Fig. 2. Double-slider mechanism: (a) simplified model and (b) force ratio vs. transmission angle.

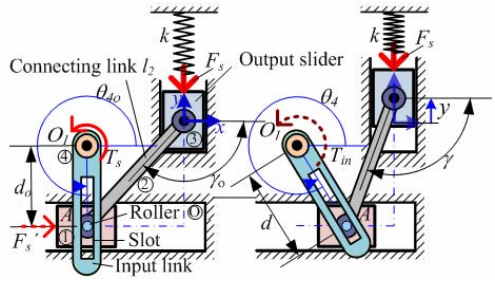

(a) (b)

Fig. 3. Double-slider mechanism with spring for realization of nonlinear stiffness: (a) zero configuration and (b) general configuration.

In this research, a new type of safety mechanism is designed and applied to an industrial manipulator. The safety mechanism is composed of linear springs and two modified double-slider mechanisms. Springs are used to absorb the collision force, while the modified double slider mechanisms determine the level of the external force. The main contribution of the proposed device is the verification of collision safety of an industrial manipulator equipped with the improved safety mechanism. The rest of the paper is organized as follows. The principle of operation is discussed in Section 2. The structure of the safety mechanism is presented in Section 3. Section 4 shows the proposed model and application of the safety mechanism. Various experimental results for both static and dynamic collisions are provided in Section 5. Finally, conclusion and future work are presented in Section 6.

2. Operational principle of safety mechanism

2.1 Feature of nonlinear stiffness

Springs are widely used for various safety mechanisms, due to their good shock absorbing properties. However, a linear spring cannot be used directly in a robot manipulator because its displacement is proportional to the external force. Fig. 1 shows that a manipulator equipped with soft springs exhibits deflection due to its own weight and/or a small load. This characteristic is advantageous to collision safety but cannot ensure positioning accuracy and repeatability because such deflections occur easily [8, 9].

The ideal nonlinear spring shown in Fig. 1 can satisfy requirements for positioning accuracy and collision safety. The stiffness of this spring is very high when the external force is within the range of normal operation; however, its stiffness rapidly drops when the external force exceeds a certain threshold level (for example, due to collision with a human or an object).

However, a spring with this ideal feature does not exist. In this study, the nonlinear power transmission characteristics of a double-slider mechanism are exploited to achieve this ideal nonlinear spring feature.

2.2 Realization of nonlinear stiffness

Nonlinear stiffness can be readily achieved using the nonlinear transmission characteristics of a four-bar linkage system. In this research, a double-slider mechanism consisting of two sliders and one connecting link is used to achieve this nonlinear spring feature.

As shown in Fig. 2(a), when an input force F_i is exerted on the input slider in the x-axis direction, an appropriate resisting force F_r acting on the output slider in the y-axis direction can maintain static equilibrium for this mechanism. In the double-slider mechanism, the transmission angle γ is defined as the angle between the connecting link and the line perpendicular to the output slider movement. The force ratio of the input to the output changes nonlinearly depending on this transmission angle, as shown in Fig. 2(b). As γ approaches 180°, a much smaller F_r is sufficient to prevent the output slider from moving for a given F_i.

To achieve the nonlinear spring characteristic shown in Fig. 1, a precompressed spring was installed between the output slider and the fixed wall as shown in Fig. 3. The spring force F_s can substitute for the input force F_r shown in Fig. 1(a), and the spring torque T_s, which induces the force F_s' to the input slider can maintain static equilibrium. By applying the principle of virtual work, the relationship between T_s and F_s is obtained as follows:

$$T_s = \frac{\delta y}{\delta \theta_4} F_s = \frac{d}{\tan\gamma \cdot \sin\theta_4} F_s \tag{1}$$

$$d = d_0 / \cos(\theta_4 - \theta_{4o}) \tag{2}$$

$$\tan\gamma = \frac{\sqrt{l^2 - \{l \cdot \sin(\gamma_0 - \pi/2) - d \cdot \sin(\theta_4 - \theta_{4o})\}^2}}{l \cdot \sin(\gamma_0 - \pi/2) - d \cdot \sin(\theta_4 - \theta_{4o})} \tag{3}$$

where γ, θ_4, and d are interconnected because this mechanism permits a 1 DOF rotation.

Consider a situation in which the input torque T_{in} is forced to

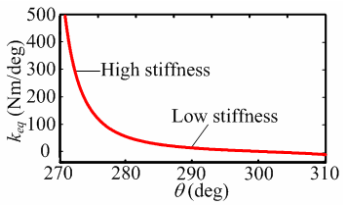

Fig. 4. Nonlinear stiffness of safety mechanism as function of angular displacement.

act on the input link (link 4 in Fig. 3). Due to the spring force caused by spring compression, the output slider does not move up until the input torque exceeds a certain threshold, thereby generating an input torque large enough to move the slider up. The input torque required to initiate movement of the output slider is defined in this study as threshold torque, T_{th}. Once the input torque exceeds this threshold, the spring is rapidly compressed until the output slider moves to the upmost position and the spring can no longer be compressed. From Eq. (1), the threshold torque can be described by

$$T_{th} = \frac{d_o}{\tan\gamma_o \sin\theta_{4o}} k s_o \tag{4}$$

where subscript o represents the zero configuration, s_o is the spring compression, d_o is the displacement between points A and O_1, θ_{4o} is the angular displacement of the input link, and k is the spring constant. From Eq. (4), the equivalent stiffness, k_{eq}, seen from the input slider can be obtained as a function of θ_4 as follows:

$$k_{eq} = \frac{d}{(\theta_4 - \theta_{4o})\tan\gamma \sin\theta_4} k(s_o + y) \tag{5}$$

where y and γ are related by $y = l_2(\sin\gamma - \sin\gamma_o)$.

Fig. 4 shows the equivalent stiffness curve as a function of angular displacement of the input slider when k=37 kN/m, s_o=12 mm, l_2=30.5 mm, θ_o=270°, and γ_o=163.5°. The equivalent stiffness k_{eq} of this nonlinear system is kept very high for a small angular displacement of the input slider, but it quickly drops as the displacement increases. Hence the nonlinear stiffness system can be realized by the double-slider mechanism combined with a precompressed linear spring.

3. Safety mechanism for industrial manipulator

3.1 Position of safety mechanism for effective collision absorption

Various types of collision can occur for an industrial manipulator with multiple degrees-of-freedom. In this study, two safety mechanisms were installed in the industrial manipulator to absorb a collision force in various directions. As shown in Fig. 5, most collisions between a human and a robot occur due to the rotation of joints 1 and 3. Therefore, the safety mechanisms were applied to these two joints to absorb collision

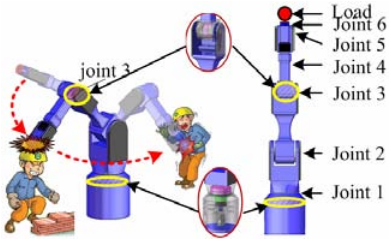

Fig. 5. Joints for safety mechanism.

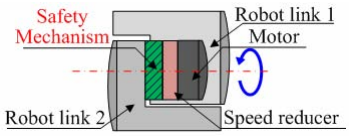

Fig. 6. Position of safety mechanism.

force. Since the safety mechanism was installed between the speed reducer and the robot link (Fig. 6), the actuator inertia from the motor and speed reducer can be decoupled from the robot link inertia in a collision.

3.2 Calculation of joint torque

The threshold torque of the safety mechanism can be set by adjusting the stiffness and initial compression of the linear spring and initial transmission angle. To obtain the positioning accuracy of a manipulator, the threshold torque should be larger than the torque required to conduct given tasks at the desired velocities and accelerations.

As shown in Fig. 5, the safety mechanisms were installed at joints 1 and 3 of a 6-DOF industrial manipulator, which has a payload of 6 kg. The capacity of each safety joint mechanism at joints 1 and 3 were determined by the operating torque. To calculate the maximum operating torque, the robot manipulator was simulated for extreme situations in which all joints moved at one time at the maximum velocity and acceleration with a payload of 6 kg. Based on the simulation, the maximum torque of joints 1 and 3 reached peak values of 40 N·m and 80 N·m, respectively. Therefore, the threshold torque of each safety mechanism was set slightly higher than these respective maximum torques.

3.3 Selection of spring stiffness

As previously mentioned, the threshold torque of the safety mechanism can be determined by the initial transmission angle, the initial compression length of the springs, and the spring stiffness. From the geometric parameters of the mechanism and the threshold torque, the spring stiffness is given by

$$k \geq \left| 0.9 \times \frac{T_{th}}{d_o \cdot s_o} \times \tan\gamma_o \right|. \tag{6}$$

Note that the coefficient of 0.9 represents the friction factor of the safety mechanism. In this design, γ_0 = 163.5°, s_o = 12 mm, and d_o = 48 mm, which yields k = 18.5 kN/m at joint 1

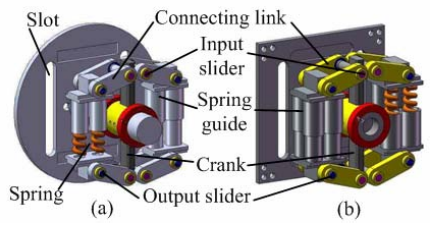

Fig. 7. Structure of safety mechanism: (a) round type for joint 3 and (b) square type for joint 1.

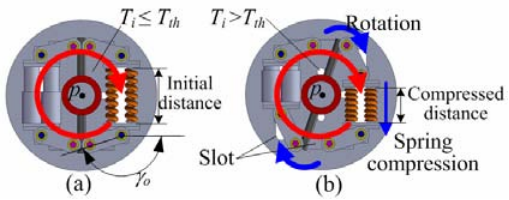

Fig. 8. Operation of safety mechanism with input torque: (a) before collision and (b) after collision.

and 37 kN/m at joint 3. To obtain sufficient compression length, low stiffness springs, each of which has a stiffness of 4.6 kN/m, were used, thus leading to four springs at joint 1 and eight springs at joint 3.

4. Design of safety mechanism

Round- and square-type safety mechanisms using the springs selected in Section 3 were designed for joints 1 and 3 of the manipulator, as shown in Fig. 7. When input torque T_i from the external load is smaller than the predetermined threshold torque T_{th}, the safety mechanism provides enough stiffness to maintain static equilibrium, which prevents rotation of the link (Fig. 8(a)). However, if the input torque exceeds the threshold torque, then the crank turns around point P, which is the center of rotation, as shown in Fig. 8(b) and the output slider is forced to move on the spring guide to compress the spring. This movement of the output slider reduces the transmission angle, so sustaining the static balance requires a greater resisting force for the same input force. However, the increased spring force, due to its compression, is not large enough to sustain this balance. This unbalanced state causes the slider to rapidly slide, and thus the collision force is absorbed by the spring compression. After the collision force is removed, the safety mechanism and manipulator can be restored to the initial state because of the stored spring energy.

Prototypes of the safety mechanism were constructed to evaluate their performance, as shown in Fig. 9. The size and weight of the square prototype are 120 x 120 x 51 mm and 1.4 kg, respectively. The size and weight of the round prototype are ϕ140 x 41 mm and 1.1 kg, respectively.

5. Experiments using safety mechanisms

To verify the performance of the safety mechanism when the manipulator collides with a human, various experimental results are presented in this section. Section 5.1 shows results which verify nonlinear stiffness and positioning accuracy. In Section 5.2, a safety criterion is proposed for the estimation of collision safety. In Section 5.3, some experiments are conducted to verify collision safety of the manipulator with and without the safety mechanism.

Fig. 9. Prototypes of safety mechanism: (a) square type and (b) round type.

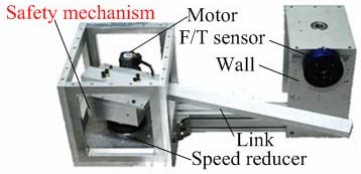

Fig. 10. Experimental setup for 1DOF robot arm with safety mechanism.

5.1 Performance test with static collision

The experimental setup shown in Fig. 10 was constructed for the evaluation of nonlinear stiffness of the safety mechanism. The safety mechanism was installed at the 1-DOF robot arm which consists of a motor, a speed reducer, and a robot link. The plate of the safety mechanism integrated with the 1-DOF robot link was attached to the gear reducer which is connected to the motor. Therefore, the motor torque can be transmitted to the robot link via the safety mechanism. An F/T sensor was installed at the wall to measure the contact force between the robot link and the wall. The contact force was converted to the corresponding joint torque in consideration of the link length of a robot arm.

The robot arm without the safety mechanism delivered a contact force up to 200 N at the wall due to high stiffness of the harmonic drive, which corresponds to the external torque of 100 Nm. However, the contact force of up to only 158 N and 78.4 N were transmitted to the wall by the robot arm with the square-type and round-type safety mechanisms, which are equivalent to the external torque of 79 Nm and 39.2 Nm, respectively, which is similar to the pre-determined threshold torque. Thus, the excessive torque was absorbed by the safety mechanism.

To evaluate the positioning accuracy of the manipulator with the safety mechanism, an experimental setup was constructed as shown in Fig. 12. The safety mechanism was installed at joint 3 of the manipulator with a load of 6 kg. The robot manipulator was forced to rotate from 60° to 90° and rotate back to its initial position. When the robot manipulator rotated 80°,

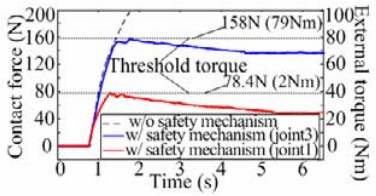

Fig. 11. Experimental results for safety mechanisms.

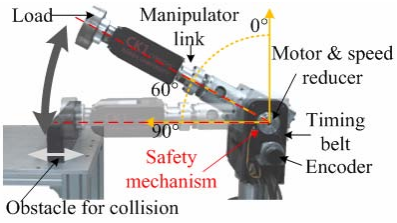

Fig. 12. Experimental setup with robot arm for repeatability test.

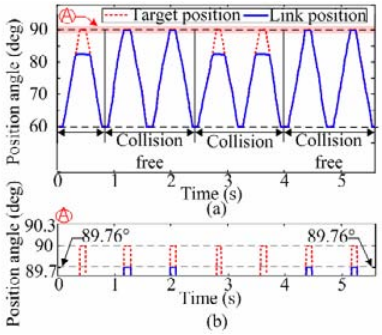

Fig. 13. Experimental results of positioning accuracy and repeatability test: (a) general view and (b) expanded view.

its end-point touched a fixed obstacle. An extra encoder was used to measure the angular displacement of the manipulator link with the safety mechanism.

The difference between the angles of the manipulator link shown in Fig. 13 was found to be nearly 0°, which is the same result as when the manipulator rotated without the safety mechanism. This means that although the safety mechanism operated to absorb the collision force, the robot manipulator with the safety mechanism provided good repeatability.

5.2 Safety criterion

Since there are no clear safety criteria associated with collision between a manipulator and a human, several different criteria have been applied to the safety evaluation. ISO 10218-1 states that the velocity and maximum static force of the flange/TCP should be less than 0.25 m/s and 150 N, respectively, and the maximum power of a robot must be less than 80 W. In [10], human pain tolerance is used as a main safety criterion, based on the observation that humans usually suffer at a contact force exceeding 50 N in a static collision. However, these safety requirements are too restrictive for a manipulator to efficiently perform the given task. The head injury criterion (HIC) and abbreviated injury scale (AIS), which were developed as safety criteria for an automobile crash, were suggested by some researchers. However, these criteria turned out to be unsuitable for manipulators whose collision speed was much lower than that of the automobile crash defined in [11].

Table 1. Fracture force of skull [13-14].

Bone	Fracture force
Frontal	4.0 kN
Temporal	3.12 kN
Occipital	6.41 kN
Mandible (center)	1.89 kN
Mandible (lateral)	0.82 kN
Zygoma	0.85 kN
Maxilla	0.62 kN
Nasal	0.34 kN

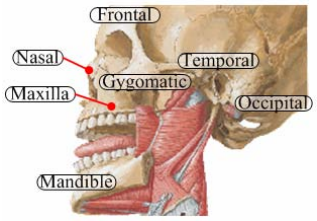

Fig. 14. Lateral surface of skull with cranial and facial bones [12].

In this study, head injury tolerance was considered because the head is the most important part of the human body. The terminology of head anatomy is illustrated in Fig. 14. Table 1 lists the fracture forces of various parts of the skull. Since the fracture forces of the maxilla and nasal region are lower than the other bones, we used these forces as our safety criterion.

5.3 Safety test for dynamic collision

To measure collision force when the robot manipulator collides with a human head, we constructed a simplified dummy model shown in Fig. 15. A bowling ball with the same size and weight as a human head was used as the dummy's head. The head was connected to the body using a linear guide and an extended tension spring to represent the stiffness of a human neck. The weight of the head and body were chosen as 6 kg and 45 kg, respectively. We considered two types of collision situations depending on the constraint condition shown in Fig. 16: unconstrained impact and constrained impact. Wheel casters were unlocked to simulate a collision for unconstrained impact, and were locked for a constrained impact. The collision force was measured by a force sensor covered with a silicon pad to mimic human skin.

As shown in Fig. 17, collision experiments were conducted for the industrial manipulator with and without the safety mechanism for constrained and unconstrained impact. In the experiment, the end point of the manipulator collided with the sensor on the ball at a constant velocity of 1 m/s. The manipulator was commanded to reach the desired position which was placed at 20° inside the ball.

Fig. 15. Experimental setup to represent human head and body for collision experiment.

Fig. 16. Types of collision: (a) constrained impact and (b) unconstrained impact.

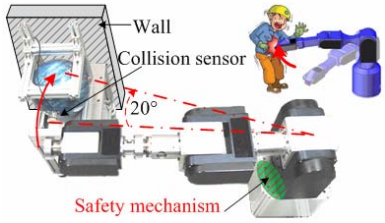

Fig. 17. Experimental setup to measure collision due to rotation of joint 1 with and without safety mechanism.

As shown in Fig. 18, for the constrained situation, the collision force of the manipulator without the safety mechanism reached a peak value 795 N which is higher than the fracture force for the maxilla and nasal bone. However, the peak value of the collision force for the robot arm with the safety mechanism was just 490 N which was less than the fracture force of a maxilla. For the unconstrained situation, the maximum collision force for the robot arm without the safety mechanism was 680 N, but just 340 N with the safety mechanism, as shown in Fig. 19.

Next, we considered the constrained situation only when collision occurs due to rotation of joint 3, as shown in Fig. 20. In this experiment, the end point of the manipulator collided at a constant velocity of 1 m/s. The manipulator was commanded to reach the desired position which was placed at 20° inside the ball.

As shown in Fig. 21, the manipulator without the safety mechanism delivered a collision force of up to 800 N to the ball, which was above the fracture force of the maxilla and the nasal bone. The collision force of the manipulator with the safety mechanism reached 620 N, which is less than the fracture force of the maxilla.

6. Conclusion

In this study, we proposed a mechanism to improve safety in collisions between humans and robot manipulators. A manipulator equipped with our safety mechanism can maintain very high stiffness up to a preset threshold torque, but provides very low stiffness above the threshold. Based on our analysis and experiments, the following conclusions are drawn:

(1) The stiffness of the manipulator abruptly drops if the external torque induced by collision exceeds the predetermined threshold torque, which improves the collision

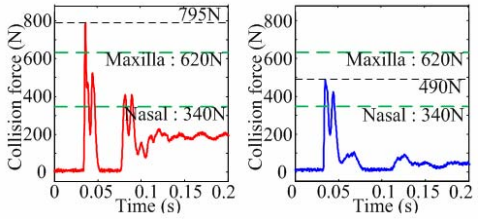

Fig. 18. Experimental results for dynamic collision under constrained situation: (a) without safety mechanism and (b) with safety mechanism.

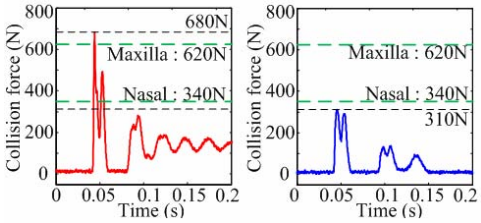

Fig. 19. Experimental results for dynamic collision under unconstrained situation: (a) without safety mechanism and (b) with safety mechanism.

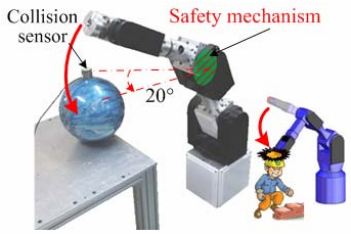

Fig. 20. Experimental setup to measure collision due to rotation of joint 3 with and without safety mechanism.

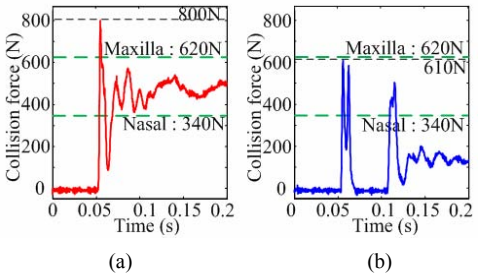

Fig. 21. Experimental results for dynamic collision under constrained situation: (a) without safety mechanism and (b) with safety mechanism.

safety of the manipulator.

(2) High stiffness of the robot manipulator can be maintained for external torque which is less than the threshold torque. Therefore, positioning accuracy can be achieved for tasks involving low external forces.

Acknowledgment

This work was supported by the Project for Development of Manipulation Technology for Human-Robot Cooperation and by the Center for Autonomous Intelligent Manipulation under Human Resources Development Program for Robot Specialists of Ministry of Knowledge Economy.

References

[1] Y. Wang and D. Zhou, S. J. Qin and H. Wang, Active fault-tolerant control for a class of nonlinear systems with sensor faults, *International Journal of Control, Automation and Systems*, 6 (3) (2008) 339-350.

[2] T. Morita and S. Sugano, Development of one-D.O.F. robot arm equipped with mechanical impedance adjuster, *Proc. of the IEEE/RSJ International Conference on Intelligent Robots and System* (1995) 407-412.

[3] M. Okada, Y. Nakamura and S. Ban, Design of programmable passive compliance shoulder mechanism, *Proc. of the IEEE International Conference on Robotics and Automation* (2001) 348-353.

[4] G. Tonietti, R. Schiavi and A. Bicchi, Design and Control of a Variable Stiffness Actuator for Safe and Fast Physical Human/Robot Interaction, *Proc. of the IEEE International Conference on Robotics and Automation* (2005) 528-533.

[5] S. Kang and M. Kim, Safe arm design for service robot, *Proc. of the International Conference on Control, Automation and System* (2002) 88-95.

[6] J.-J. Park, B.-S. Kim, J.-B. Song and H. S. Kim, Safe link mechanism based on nonlinear stiffness for collision safety, *Mech. Mach. Theory,* 43 (10) (2008) 1332-1348.

[7] J.-J. Park, Y.-J. Lee, J.-B. Song and H. S. Kim, Safe joint mechanism based on nonlinear stiffness for safe human-robot collision, *Proc. of the IEEE International Conference on Robotics and Automation* (2008) 2177-2182.

[8] V. P. Phan, N.-S. Goo and H.-C. Park, Vibraion suppression of a flexible robot manipulator with a lightweight piezo-composite actuator, *International Journal of Control, Automation and Systems*, 7 (2) (2009) 242-252.

[9] J. H. Yoo, M. W. Hyun, J. H. Choi, S. C. Kang and S. J. Kim, Optimal design of a variable stiffness joint in a robot manipulator using the response surface method, *Journal of Mechanical Science and Technology* 23 (8) (2009) 2236-2243.

[10] Y. Yamada, Y. Hirasawa, S. Y. Huang and Y. Umetani, Fail-safe human/robot contact in the safety space, *IEEE International Workshop in Robot and Human Communication* (1996) 59-64.

[11] S. Haddadin, A. Albu-Schaffer and G. Hirzinger, The role of the robot mass and velocity in physical human-robot interaction-Part I: Non-constrained blunt impacts, *IEEE International Conference on Robotics and Automation* (2008) 1331-1338.

[12] N. S. Norton, Netter's head and neck anatomy for dentistry, (2006) 430.

[13] SAE J885 APR 80, 1980, Human tolerance to impact conditions as related to motor vehicle design.

[14] A. M. Nahum, Impact studies of facial bones and skull, Proc. of the 16th Stapp Car Crash Conference (SAE Technical Paper No. 720965) (1972) 8-10.

Hwi-Su Kim received his B.S. degree in Mechanical Engineering from Korea University, in 2007. He is now enrolled in the Integrated Master's & Doctoral course in Mechanical Engineering at Korea University. His research interests include manipulator design and safe robot arms.

Jung-Jun Park received his M.S. and Ph.D. degree in Mechanical Engineering from Korea University, in 2005 and 2010, respectively. Dr. Park is currently engaged in postdoctoral work in the School of Mechanical Engineering at Korea University. His research interests include robotic manipulation and safe robot arms.

Jae-Bok Song received his B.S. and M.S. degree in Mechanical Engineering from Seoul National University in 1983 and 1985, respectively. He was awarded his Ph.D. degree from M.I.T. in 1992. Dr. Song is currently a Professor at the School of Mechanical Engineering at Korea University. He has served as a director of Intelligent Robotics Laboratory from 1993. Dr. Song's research interests include safe manipulators, design and control of robotic systems, and indoor/outdoor navigation.

Jin-Ho Kyung received his B.S. and M.S. degree in Mechanical Engineering from Korea Aerospace University and KAIST in 1985 and 1988, respectively. He was awarded his Ph.D. degree from KAIST in 2003. Dr. Kyung is currently a Principal Researcher at Dept. of Robotics & Intelligent Machinery at Korea Institute of Machinery and Materials, and he has served as a head of Robot team. Dr. Kyung's research interests include the design and control of robotic systems, and manipulation technology for human-robot cooperation.